routing; search and rescue; antisubmarine warfare and surveillance; tactical planning; high-resolution boundary conditions for even higher resolution coastal models; inputs to ice, atmospheric, and bio-physical models and shipboard environmental products; environmental simulation and synthetic environments; observing system simulations; ocean research; pollution and tracer tracking; and inputs to water quality assessment.

[Sponsored by ONR and SPAWAR]

References

[1] S.L. Cross and J. Schmitz, "Navy Layered Ocean Model: The First 100 Days," *NAVO Bull.*, 1, 4-5, Aug. 2000.

[2] E.P. Chassignet, Z.D. Garraffo, R.D. Smith, and H.E. Hurlburt, "High-resolution Gulf Stream Modeling," *Geophy. Res. Lett.* (submitted) (2000).

[3] H.E. Hurlburt and P.J. Hogan, "Impact of 1/8° to 1/64° Resolution on Gulf Stream Model—Data Comparisons in Basin-scale Subtropical Atlantic Ocean Models," *Dyn. Atmos. Ocean.* **32**, 283-329 (2000).

[4] H.E. Hurlburt, A.J. Wallcraft, W.J. Schmitz, Jr., P.J. Hogan, and E.J. Metzger, "Dynamics of the Kuroshio/Oyashio Current System Using Eddy-resolving Models of the North Pacific Ocean," *J. Geophys. Res.* **101**, 941-976 (1996).

[5] H.E. Hurlburt, R.C. Rhodes, C.N. Barron, E.J. Metzger, O.M. Smedstad, and J.-F. Caynla, "A Feasibility Demonstration of Ocean Model Eddy-resolving Nowcast/Forecast Skill Using Satellite Altimeter Data," NRL/MR/7320--00-8235, 23 pp. (2000).

[6] Office of Science and Technology Policy, "Appendix A: Summary of Grand Challenges," in *The Federal High Performance Computing Program*, Executive Office of the President (1989).

[7] A.J. Wallcraft and D.R. Moore, "The NRL Layered Ocean Model," *Parallel Comput.* **23**, 2227-2242 (1997).

Bimodal Directional Distribution of the Second Kind: Resonant Propagation of Wind-Generated Ocean Waves

P.A. Hwang,[1] D.W. Wang,[1] W.E. Rogers,[1]
J.M. Kaihatu,[1] J. Yungel,[2] R.N. Swift,[2]
and W.B. Krabill[3]
[1]*Oceanography Division*
[2]*EG&G*
[3]*NASA*

Introduction: Over the last several decades, it has been accepted that under steady forcing, wind-generated waves travel in the direction of wind. Last year, we presented two-dimensional (2D) spectral analysis of 3D ocean wave topography at equilibrium stage.[1] The results demonstrate unequivocally a robust bimodal directionality in wave components shorter than the dominant wavelength. The generation mechanism of the bimodality is clarified to be nonlinear wave-wave interaction. Continued investigation reveals a second kind of bimodal directional distribution produced by resonant propagation of waves with the forcing wind field. In this situation, the *dominant* waves in a young sea align in oblique angles with the wind direction to maintain propagation resonance for a more efficient air-sea momentum transfer. As a result, two symmetric wave systems straddle the wind vector. The results from these analyses will revise our fundamental understanding of the physics of wind-wave generation and the forcing functions governing the dynamics of ocean waves. The implications of these directional observations on remote sensing (directional characteristics of ocean surface roughness) and air-sea interaction (directional properties of mass, momentum, and energy transfers) are significant.

Airborne Observation and Analysis: Reference 1 reports spatial measurements of ocean waves using an airborne topographic mapper (ATM, an airborne scanning lidar system). The 3D topography provides an excellent directional resolution. Figure 8 shows images of the wave conditions at three different fetches along a flight track in the Gulf of Mexico. The waves are generated by a steady offshore wind following a cold front passing through the region. The top image (Fig. 8(a)) is in the near-shore region, and the coastline is visible in the image. The orientation of the surface undulations is perpendicular to the wind. The next two images (Figs. 8(b)-(c)) are farther downwind. The crosshatched patterns suggest that two wave systems of about equal intensity are crossing each other at a large angle. It is quite obvious that these wave patterns do not fit the conventional unimodal directional distribution function, which has been assumed explicitly or implicitly in the description of surface roughness properties relating to remote sensing and air-sea transfers.

Recent advances in global positioning, laser ranging, and computer technologies provide the capability to acquire high-resolution topography of ocean surface waves for quantitative analysis of their spatial and temporal evolutions. Figure 9(a) shows a sequence of surface wave topography over the 42-km flight track, along which the three photographs shown in Fig. 8 were taken. The corresponding directional wavenumber spectra are shown on the right-hand side of the figure (Fig. 9(b)). The dominant waves of this sequence of spectra are obviously directionally bimodal. At short fetches, the dominant wave direction is crosswind rather than along-wind. As fetch increases, two distinct wave systems propagate obliquely to the wind, forming a crosshatched pattern (Fig. 9(a)). These are characteristics of resonant propa-

Report Documentation Page

Form Approved
OMB No. 0704-0188

1. REPORT DATE	2. REPORT TYPE	3. DATES COVERED
2001		**00-00-2001 to 00-00-2001**

4. TITLE AND SUBTITLE	5a. CONTRACT NUMBER
Bimodal Directional Distribution of the Second Kind: Resonant Propagation of Wind-Generated Ocean Waves	5b. GRANT NUMBER
	5c. PROGRAM ELEMENT NUMBER
6. AUTHOR(S)	5d. PROJECT NUMBER
	5e. TASK NUMBER
	5f. WORK UNIT NUMBER
7. PERFORMING ORGANIZATION NAME(S) AND ADDRESS(ES) **Naval Research Laboratory,Oceanography Division,4555 Overlook Avenue, SW,Washington,DC,20375**	8. PERFORMING ORGANIZATION REPORT NUMBER
9. SPONSORING/MONITORING AGENCY NAME(S) AND ADDRESS(ES)	10. SPONSOR/MONITOR'S ACRONYM(S)
	11. SPONSOR/MONITOR'S REPORT NUMBER(S)

12. DISTRIBUTION/AVAILABILITY STATEMENT
Approved for public release; distribution unlimited

13. SUPPLEMENTARY NOTES

14. ABSTRACT

15. SUBJECT TERMS

16. SECURITY CLASSIFICATION OF:			17. LIMITATION OF ABSTRACT	18. NUMBER OF PAGES	19a. NAME OF RESPONSIBLE PERSON
a. REPORT **unclassified**	b. ABSTRACT **unclassified**	c. THIS PAGE **unclassified**	**Same as Report (SAR)**	**3**	

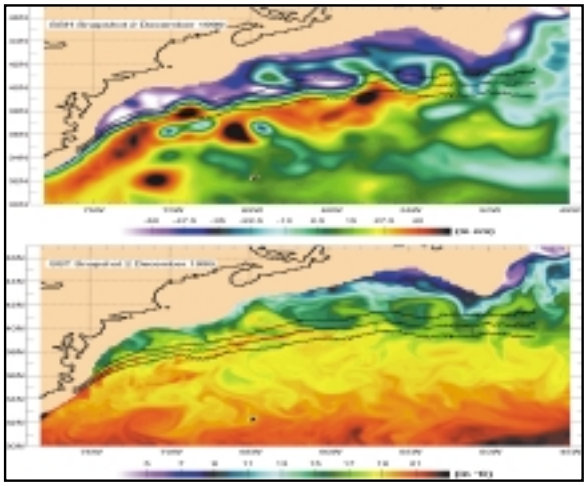

FIGURE 8
Ocean surface waves produced by a steady offshore wind. The fetch (distance from shore) increases from top to bottom.

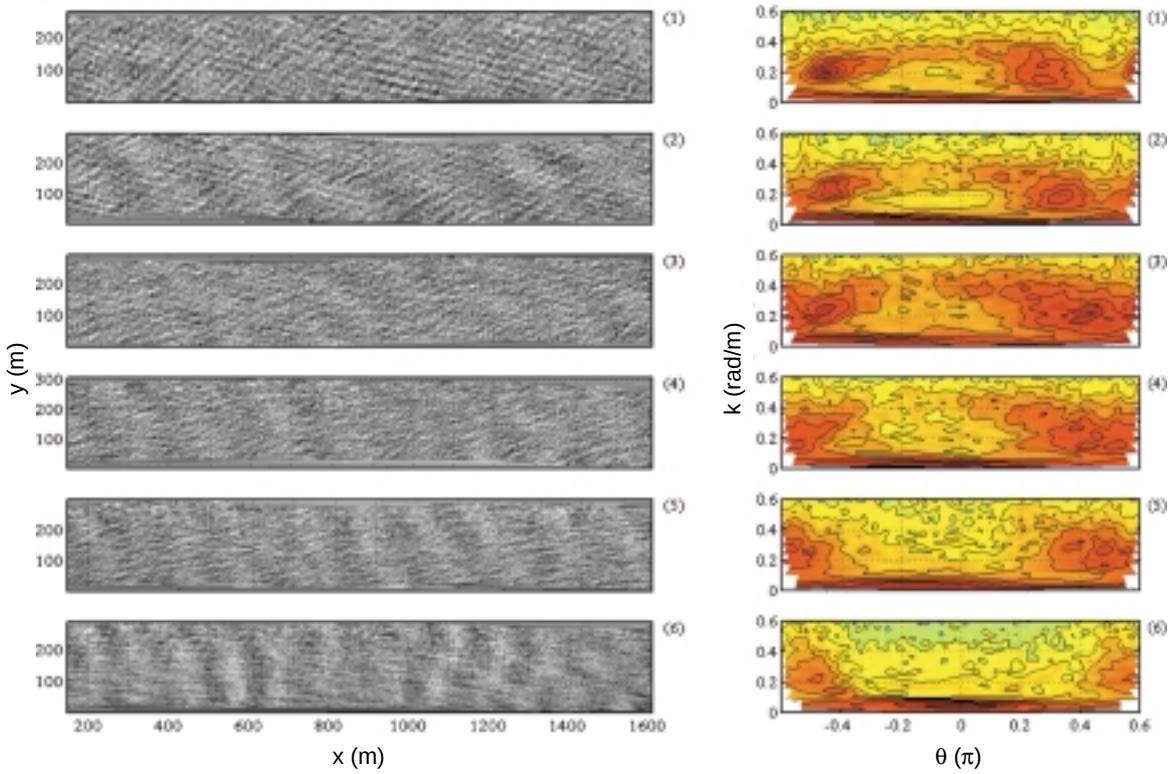

FIGURE 9
(a) 3D surface topography of ocean waves along a flight track at 6 different fetches (38.1, 31.5, 24.8, 18.2, 11.5, and 4.93 km from top to bottom). The wind is blowing from right to left. (b) The corresponding 2D spectra calculated from the surface topographies shown in (a). The wind direction is at θ = 0°.

gation between winds and waves. Under the resonant condition, waves propagate in step with the wind field to receive continuous nourishment from the wind. Because the phase velocity of young waves is much slower than the wind speed, to maintain propagation resonance, they travel at oblique angles from the wind. Reference 2 provides details of the analysis on the spatial and temporal evolution of wind-generated waves.

Summary: It has been held as common knowledge that wind-generated waves propagate in the direction of the wind. This concept has been incorporated into unimodal directional distribution functions in virtually all spectral wave models, as well as in the wind input function in the equation governing the dynamics of ocean surface waves. Recent field measurements of 3D ocean surface topography, however, do not support the assumption. The analysis of 3D wave topography indicates that the directional distribution of ocean surface waves is primarily bimodal. Two different kinds of directional bimodality are confirmed. The first kind, bimodality, occurs at the equilibrium stage and in wave components shorter than the dominant wavelength. The physical mechanism is nonlinear wave-wave interaction that distributes energy from near the spectral peak toward oblique components, forming a resonant quartet. The second kind, bimodality, occurs at the young stage and on dominant waves. The generation mechanism is resonant propagation between winds and waves.

[Sponsored by ONR.]

References

[1] P.A. Hwang, D.W. Wang, E.J. Walsh, W.B. Krabill, W. Wright, and R.N. Swift, "Airborne Measurements of the Directional Wavenumber Spectra of Ocean Surface Waves. Part 2. Directional Distribution," *J. Phys. Oceanogr.* **30**, 2768-2787 (2000).

[2] P.A. Hwang, D.W. Wang, W.E. Rogers, J. Yungel, R.N. Swift, and W.B. Krabill, "Bimodal Directional Propagation of Wind-generated Ocean Waves," *J. Phys. Oceanogr.* (submitted) (2000).

A Video-Based Particle Image Velocimetry (PIV) Technique for Nearshore Flows

J.A. Puleo, K. Holland, and T.N. Kooney
Marine Geosciences Division

Introduction: Natural beaches undergo constant change as they are forced by local physical processes (such as waves and currents) and human-induced processes (such as nourishment or structure development). In addition to scientific and societal interest, beach or nearshore extreme conditions can also be important for military operations relating to amphibious landings and mine burial. While no accurate model exists to predict beach change, it is generally accepted that nearshore (littoral) processes such as beach erosion are largely forced by waves and current variability. Of these two processes, the current field is most difficult, given that flows in this region are typically very complex and nonuniform in space and time. The traditional approach involves in situ instrumentation, but, due to cost and logistics difficulty in placing instruments in the dynamic nearshore, deployments tend to be extremely sparse. An alternate method to standard instrumentation is needed to densely and accurately record nearshore flow phenomena.

Particle Image Velocimetry (PIV): Recently, a video-based remote sensing technique was developed at the Naval Research Laboratory for quantifying nearshore flow fields using particle image velocimetry (PIV).[1] PIV is a nonintrusive technique to extract nearly instantaneous flow fields by correlating sequential images of a passive, tracer-laden flow. Here, we use foam patterns caused by breaking waves and bores as they move across the nearshore region and the subsequent motion of the foam by local currents.

Synthetic Example: Figure 10 shows two synthetic sequential images separated in time by Δt. The offset between Fig. 10(b) and Fig. 10(a) was manually introduced as 7 pixels to the right and 4 pixels down. Up to 15% noise at each pixel location was also introduced to both images. The overlain grid of nodes (blue dots) is where velocity vectors are to be evaluated. For a given grid node, a collection of pixels I is selected from the first image and repeatedly compared using an error correlation function (very similar to cross correlation) to search windows S of the same size as I in the second image. The maximum correlation is then determined such that the spatial offsets Δx and Δy and the time separation yield the horizontal velocity components as $u = \Delta x/\Delta t$ and $v = \Delta y/\Delta t$. The magenta vectors in Fig. 10(b) are those returned from the PIV routine and correspond to the manual offsets introduced to the images. In the field, swash zone foam patterns are captured via video camera, digitized, and then geo-rectified[2] to a real-world coordinate system before PIV application.

Swash Zone Flows: Figure 11 shows two examples of the PIV technique applied to video data